

1 **Assessment and optimization of a single flash geothermal system recovered**
2 **by a trans-critical CO₂ cycle using different scenarios**

3 Yashar Aryanfar¹, Siamak Hoseinzadeh², Mario Lamagna², Benedetto Nastasi², Davide Astiaso Garsia²,
4 Soheil Mohtaram³, HongGuang Sun^{1*}

5 ¹ State Key Laboratory of Hydrology-Water Recourses and Hydraulic Engineering, International
6 Center for Simulation Software in Engineering and Sciences, College of Mechanics and Materials,
7 Hohai University, Nanjing 210098, Jiangsu, China

8 ² Department of Planning, Design, and Technology of Architecture Sapienza University of Rome,
9 Rome 00196, Italy

10 ³ School of Energy and Power Engineering, University of Shanghai for Science and Technology,
11 Shanghai 200093, China

12 **Abstract:** Globally, the use of renewable energy, particularly geothermal energy, is rising
13 quickly. Geothermal cycles' low efficiency has repeatedly shown how crucial it is to recover
14 heat lost during these cycles. This study suggests a combined power generation cycle
15 replicating using the EES software environment that combines a single flash cycle with a trans-
16 critical carbon dioxide cycle. The findings demonstrate that, in comparison to the BASIC single
17 flash cycle, the design characteristics of the proposed system are greatly improved. The
18 suggested strategy is then enhanced by employing the genetic algorithm, the Nelder-Mead
19 Simplex method, and the direct algorithm. Separator pressure, steam turbine outlet pressure,
20 and carbon dioxide turbine inlet pressure are three assumed variable parameters, and exergy
21 efficiency is the target parameter. In the default operating mode, the system exergy efficiency
22 is 32.46%, increasing to 39.21% using the genetic algorithm and 36.16% using the Nelder-
23 Mead method and 38.82% using the direct algorithm.

24 **Keywords:** Optimization, Single flash Geothermal, Genetic Algorithm, Nelder-Mead Simplex, Direct
25 Algorithm, trans-critical CO₂ cycle

26 1. INTRODUCTION

27 The planet's population is increasing yearly, and energy needs are increasing daily. The most
28 important source of human energy in the world is fossil fuels. However, fossil fuel sources are
29 not renewable and bring important environmental risks [1]. In recent years, the environmental
30 effects caused by fossil fuels have become more visible. Global warming has led to the melting
31 of the polar ice caps and endangered all creatures' lives. Also, natural fires and storms have
32 caused irreparable dangers. For this reason, alternative and clean energy sources for fossil fuels
33 have received much attention in recent years. Solar, wind, water, fuel cell, geothermal and
34 biomass energies are among the renewable energies [2]. Choosing a clean energy production
35 method depends on various factors, including geographical and biological conditions and
36 operating costs. In addition, energy conversion processes must be free of environmental
37 hazards, and their adverse effects, such as the production of extreme heat and the release of
38 environmental pollutants, must be avoided. Choosing a clean energy production method
39 depends on various factors, including geographical and biological conditions and operating
40 costs [3]. In addition, energy conversion processes must be free of environmental hazards, and
41 their adverse effects, such as the production of extreme heat and the release of environmental
42 pollutants, must be avoided. Among the clean energy production methods, the use of wind and
43 water energy has the lowest cost, and the use of solar energy has the highest cost. Due to some
44 advantages, geothermal energy is one of the suitable options for renewable energy production.
45 Unlike other renewable energies, geothermal energy is not limited to specific seasons, times
46 and conditions and can be used without interruption. Also, the cost of electricity in geothermal
47 power plants is competitive with other common (fossil) power plants and is even cheaper than
48 other new energy types. Therefore, geothermal resources are of particular importance due to
49 their availability, simple technology for creating power plants, the possibility of uninterrupted
50 operation and long-term use [4].

51 The heat extraction capabilities of the N₂O, CO₂, and H₂O EGS¹ were analyzed and compared
52 by Liu et al. [5]. A two-dimensional thermo-hydraulic-mechanical (THM) coupled EGS model
53 with discrete fractures is established. The effects of the injection-production parameters on the
54 heat extraction outcomes of the EGS with various working fluids are also examined. According
55 to the findings, N₂O-EGS and CO₂-EGS perform nearly identically in heat extraction under the
56 same circumstances. Sahana et al. [6] investigated a supercritical CO₂ power cycle proposed to
57 recover the heat of the hot water obtained at a temperature close to 140 °C from the oilfield in
58 the HWCS. An ejector expansion CO₂ refrigeration cycle uses the output power of the
59 supercritical CO₂ power cycle to run its compressor. The HDH (Humidification-
60 dehumidification) desalination unit partially uses the rejected heat of CO₂ cycles. A coupled
61 thermal model for this system is proposed by Liao et al., considering the coupling effects of
62 temperature and pressure on CO₂ flow and heat transfer. According to the simulation results,
63 at 230 m of well separation, the thermal breakthrough time is roughly 40 days. Wang et al. [7]
64 ran simulations of geothermal heat mining using supercritical CO₂ (sCO₂) in this study.
65 Subcritical, superheated, and supercritical organic Rankine cycles (ORCs) working fluid
66 selection criteria are then provided for power generation using sCO₂ from a geothermal
67 reservoir. A working fluid classification method for ORC is being proposed in the meantime.
68 Jiang et al. [8] used models to forecast the system efficiencies for the two standalone and hybrid
69 systems. Compared to standalone CO₂-EGS and CO₂-solar thermal systems, it has been
70 discovered that the hybrid system has an efficiency that is on par with or even higher than the
71 combined efficiency of the two individual systems.

72 This research calculates a power generation system's energy and exergy efficiency using a
73 combined single flash geothermal source with a trans-critical carbon dioxide cycle. Essential
74 performance parameters, including separator pressure, the inlet pressure of the carbon dioxide

1 Enhanced Geothermal System

75 turbine and the steam turbine outlet pressure, will be examined to determine the optimum
76 operating point. The novelty of the present work is the optimization of the main parameters of
77 the recovery system to achieve the maximum possible efficiency by simultaneously using the
78 genetic algorithm and Nelder-Mead simplex method. The main aims of this research are:
79 - Modeling a single flash geothermal power plant powered by a transcritical CO₂ Cycle
80 - Optimize the system based on the GA² and NMS³ and DA⁴ methods, find the best system
81 performance and maximize efficiencies.
82 - Comparison of optimization results of the algorithms and method used to identify more
83 effective optimization tools.
84 - Studying changes in energy efficiency, exergy, and total output power relative to the basic
85 parameters of the system.

86

87 **2. Proposed system description**

88 Figures 1(a) and 2(a) depict the basic single-flash geothermal cycle and single-flash geothermal
89 cycle powered by the trans-critical carbon dioxide cycle that has been suggested. Also, Figure
90 1(b) shows the temperature-entropy diagram of the single flash geothermal basic cycle. Also,
91 Figure 2(b) presents the temperature-entropy diagrams of the single flash section, and Figure
92 2(c) presents the temperature-entropy diagram of the trans-critical carbon dioxide section in
93 the proposed recovery system. Software called Engineering Equation Solver (EES) was used
94 to simulate the system. In the simulation technique, each system component is used as a control
95 volume engineering, and the first and second laws of thermodynamics are applied to it.

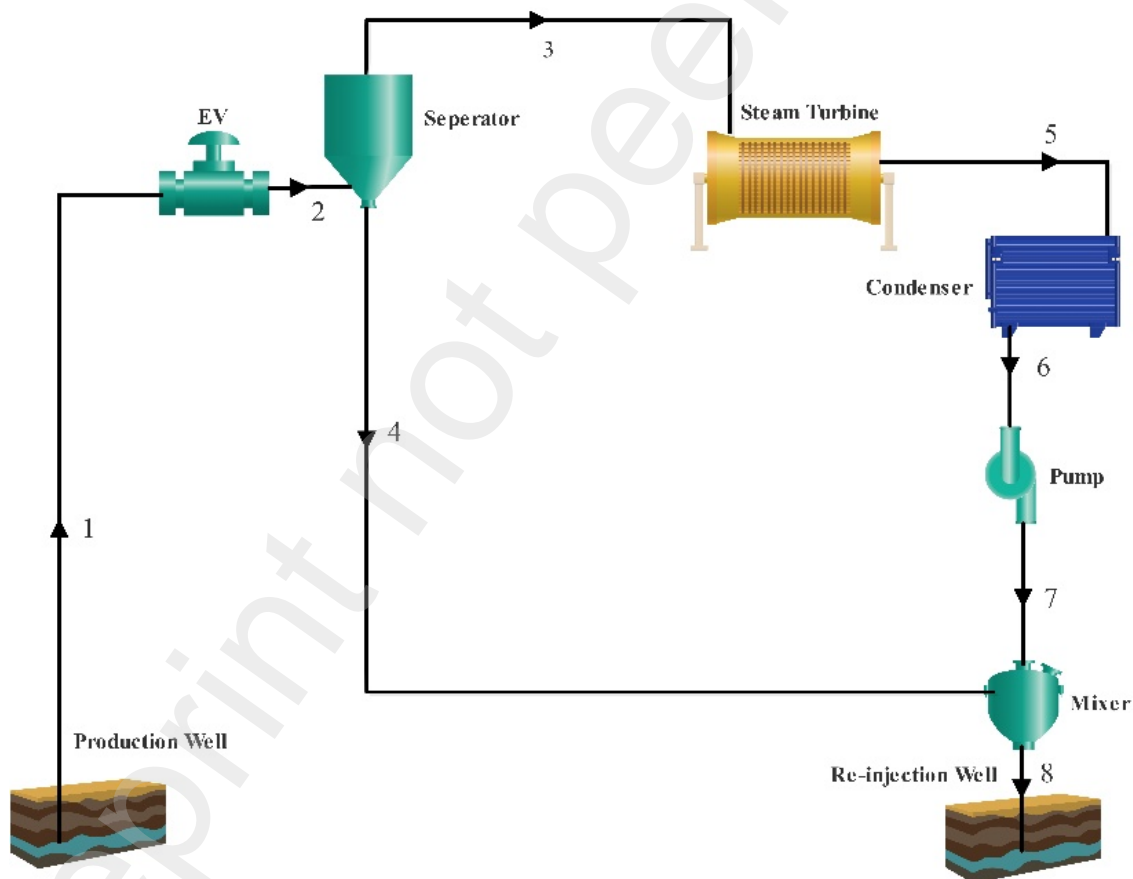
96 As shown in Figure 2(a), some geothermal fluid that has entered the system is transformed into
97 two-phase fluid during the decompression process, in which the pressure drop occurs at a

² Genetic Algorithm

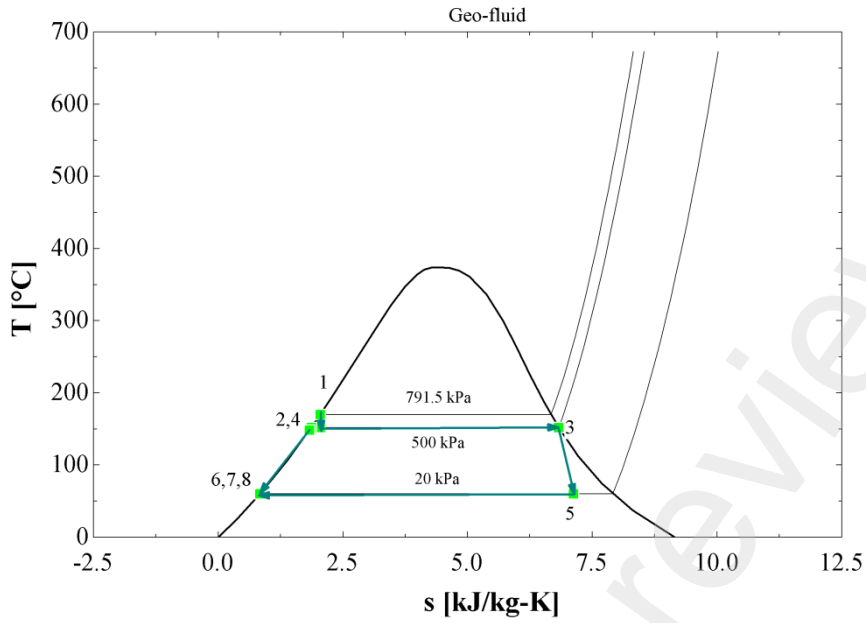
³ Nelder-Mead Simplex

⁴ Direct Algorithm

98 constant enthalpy. The two-phase fluid then enters the separator, where the saturated vapor part
 99 of the fluid generates energy in the steam turbine. Before the heat exchanger's outlet fluid is
 100 returned to the ground, the saturated liquid section of the separator also enters the vapor
 101 generator (VG), which elevates the temperature of carbon dioxide gas. It enters the gas turbine
 102 at the right temperature and pressure, producing more power for the entire system. This
 103 research differs from past investigations because it incorporates a heat exchanger into the
 104 carbon dioxide cycle. The system's performance is enhanced by this heat exchanger, which
 105 warms the incoming gas to the vapor generator using the heat of the output fluid from the
 106 single-cycle steam turbine. The output fluid of the steam turbine is sent to the re-injection well
 107 after going through the heat exchanger and cooling in a condenser.



108
 109 Figure 1(a). Schematic of basic single flash geothermal power plant.

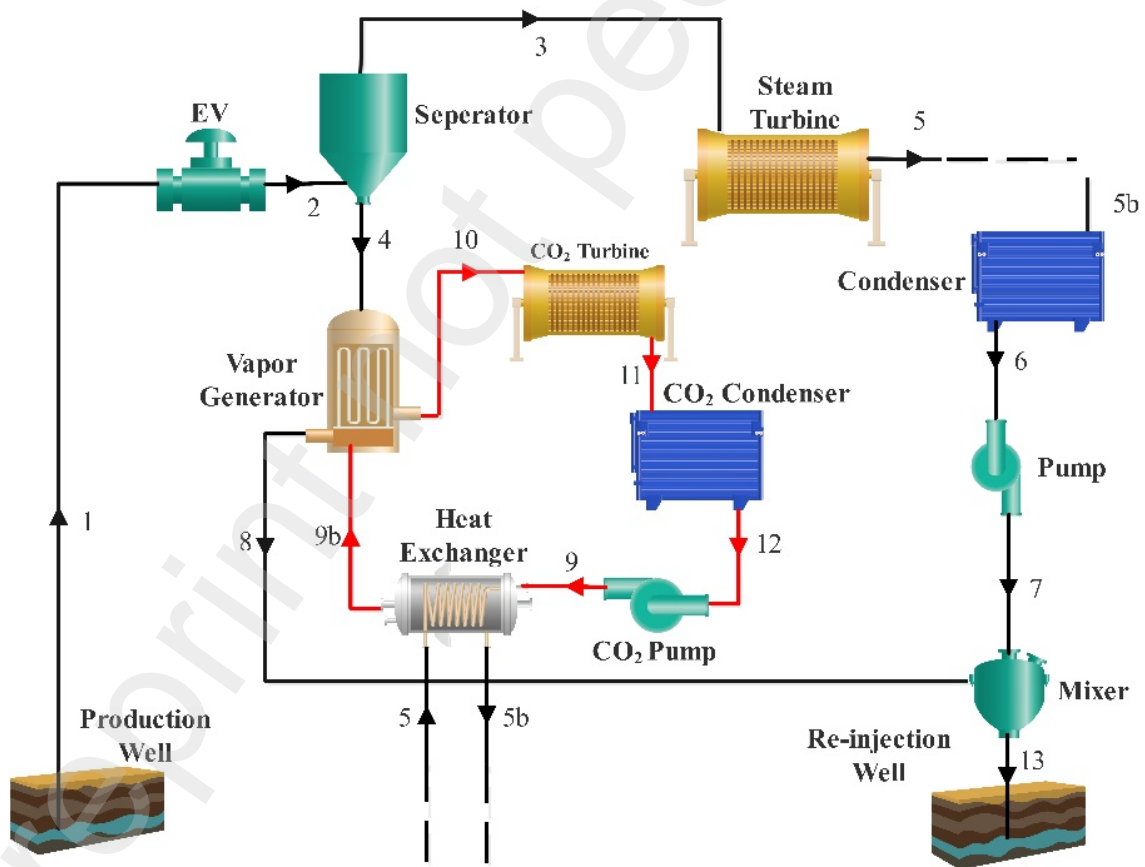


110

111

Figure 1(b). Single flash geothermal power plant T-S diagram.

112



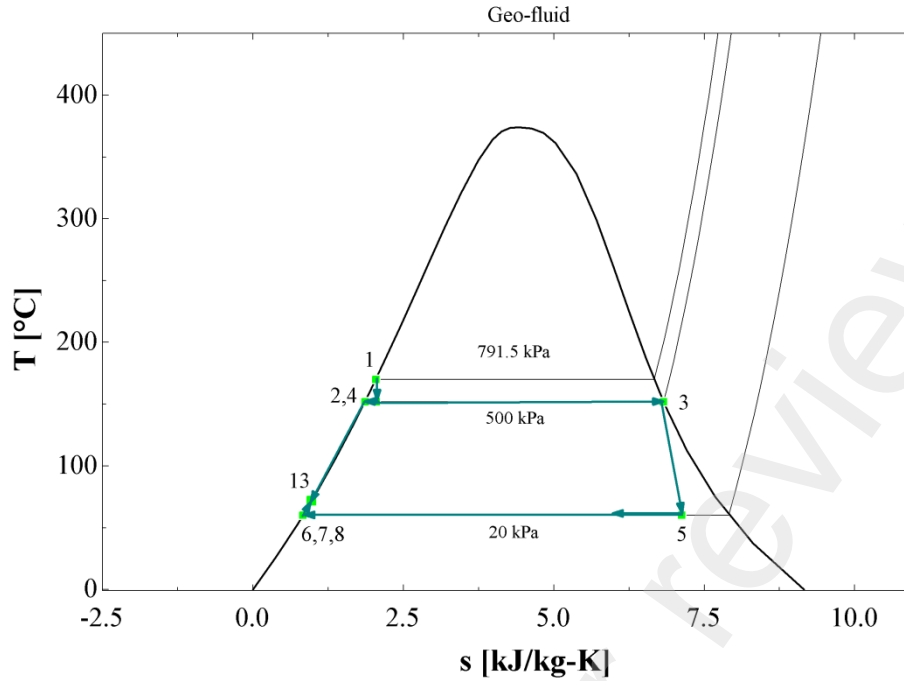
113

114

Figure 2(a). Schematic of single flash geothermal power plant powered by a trans-critical

115

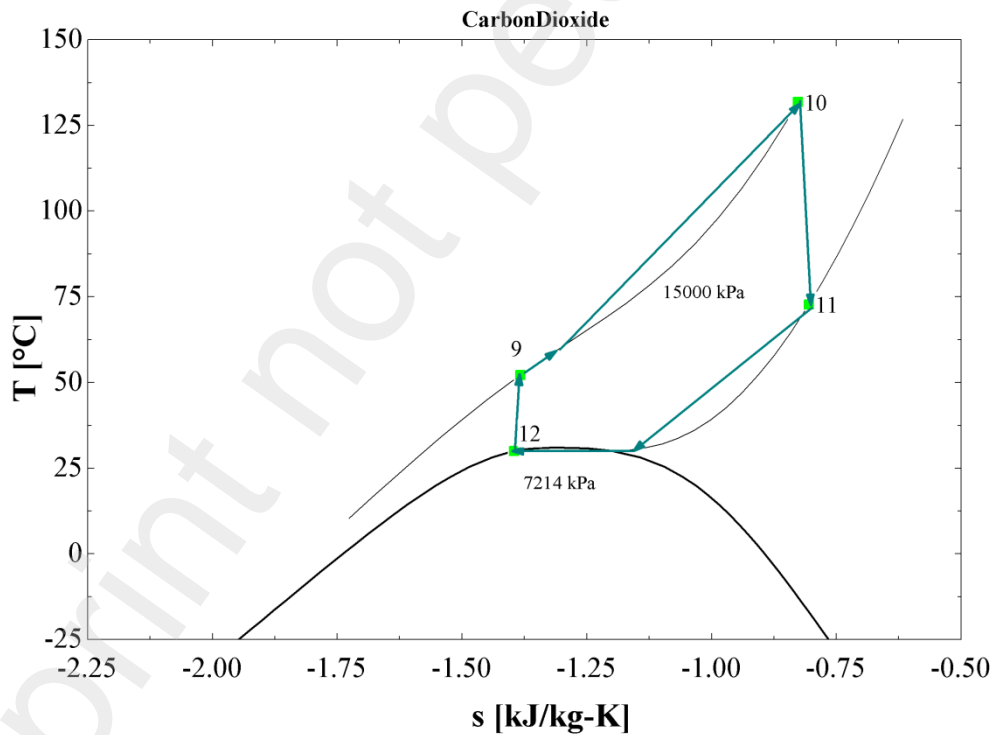
CO₂ cycle.



116

117

Figure 2(b). Single flash geothermal power plant T-S diagram in the recovery mode.



118

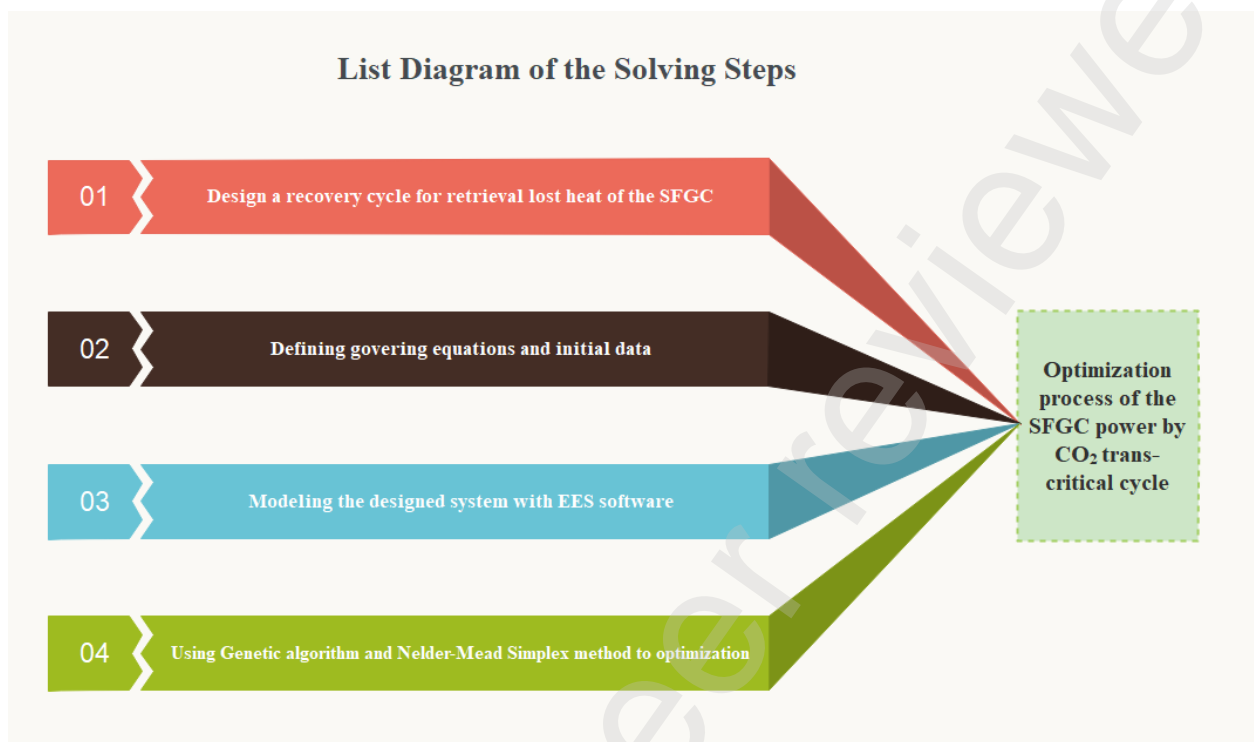
119

Figure 2(c). T-S diagram of trans-critical CO₂ cycle in the recovery mode.

120 Finding the congestion point in a trans-critical cycle is challenging since the temperature

121 change's slope fluctuates as carbon dioxide gas warms up inside heat exchangers like an

122 evaporator. The temperature difference between the beginning and end is treated as constant
123 for ease of solution.



124

125 Figure 3. List Diagram of the problem solution process

126 Figure 3 shows the list diagram of the research steps. According to Figure 3, in the present
127 work, in the first step, the primary single flash geothermal cycle and recovery trans-critical
128 CO₂ cycle are designed to recover dissipated heat. In the second step, the initial data, and
129 governing equations of the systems under study are defined using the research literature. The
130 proposed recovery system is simulated in the EES software environment in the third step. In
131 the last step, the results are optimized using genetic algorithms, the Nelder-Mead Simplex
132 method, and the direct algorithm.

133

134 3. Governing Equations

135 According to equations (1) and (2) and neglecting kinetic and potential energies, the system is
136 written while considering the control volume, mass, and energy balances for each component
137 of the system (2) [9-13]:

$$\Sigma \dot{m}_i = \Sigma \dot{m}_o \quad (1)$$

$$\Sigma \dot{Q} + \Sigma \dot{m}_i h_i = \Sigma \dot{m}_o h_o + \dot{W} \quad (2)$$

138 Equations (3) and (4) will yield the isentropic efficiency and net power production of each
139 turbine:

$$\eta_{Tur} = \frac{h_i - h_o}{h_i - h_{o,s}} \quad (3)$$

$$\dot{W}_{Tur} = \dot{m}_i (h_i - h_o) \quad (4)$$

140 The isentropic efficiency and net power of each pump are represented as follows:

$$\eta_{Pump} = \frac{h_i - h_{o,s}}{h_i - h_o} \quad (5)$$

$$\dot{W}_{Pump} = \dot{m}_i (h_o - h_i) \quad (6)$$

141 Equations (7), (8), and (9) will represent the net power of the system as well as the energy
142 efficiency and exergy efficiency of the entire system [14-16]:

$$\dot{W}_{net} = \dot{W}_{tur,steam} + \dot{W}_{tur,CO2} - \dot{W}_{pump,steam} - \dot{W}_{pump,CO2} \quad (7)$$

$$\eta_{en} = \dot{W}_{net} / \dot{Q}_{in} \quad (8)$$

$$\eta_{ex} = \dot{W}_{net} / E_{in} \quad (9)$$

143 In the current investigation, the following hypotheses are considered [17-19]:

- 144 1. All cycle parts function in steady-state situations (as a control volume).
- 145 2. Changes in kinetic energy and potential in all components are insignificant, and
146 pressure drop and heat loss in pipelines can be disregarded.
- 147 3. The isotropic efficiency of pumps is 0.75, while that of turbines is 0.8.
- 148 4. The ambient temperature and pressure for the analysis that is being presented are 25 °C
149 and 0.1 MPa, respectively.

150 Table 1. Initial data for modelling [14]

Definition	Values
------------	--------

Ambient temperature (T_0)	25 °C
Ambient Pressure (P_0)	100 kPa
Geothermal fluid inlet temperature (T_1)	170 °C
Geo-fluid mass flow rate (\dot{m}_1)	10 kg/s
Geo-fluid inlet pressure (P_1)	Saturated
Separator pressure (P_2)	500 kPa
Steam turbine output pressure (P_5)	20 kPa
CO₂ turbine inlet pressure (P_{10})	15000 kPa
CO₂ condenser temperature (T_{cond})	30 °C
Turbine isentropic efficiency (η_{tur})	0.8
Pump isentropic efficiency (η_{pump})	0.75
Evaporator inlet-outlet difference temperature (ΔT_{TTD})	20 °C
Heat Exchanger Pinch Point (ΔT_{PP})	5 °C

151 In this section, the suggested system's performance is assessed and analyzed, and the tables
152 reflect the findings of energy optimization and exergy. The input parameter values are listed in
153 Table 1 to examine the impact of various parameters on the system performance. The separator
154 pressure and the difference between the evaporator tightening point temperature and the
155 evaporator temperature determine the net output power, thermal efficiency, and exergy
156 efficiency for the cycles under study. For optimization, we will have equations (10) to (13):

$$F = \eta_{ex}(P_2, P_5, P_{10}) \quad (10)$$

$$200 < P_2(kPa) < 800 \quad (11)$$

$$12000 < P_{10}(kPa) < 18000 \quad (12)$$

$$10 < P_5(kPa) < 40 \quad (13)$$

158 **4. Results and discussions**

159 The genetic algorithm (GA) is a popular metaheuristic technique for optimizing stated
160 functions in a confined area. According to the algorithm's inheritance, past information is
161 retrieved and employed in the search process. In 1989, Goldberg invented the principles of the
162 genetic algorithm. An Evolutionary Guideline is the simulation approach described below. The
163 Evolutionary Guideline simulation technique is a neighborhood search strategy that works the
164 same way as a gene does [20].

165 Furthermore, The Nelder–Mead Simplex method, first published in, is a commonly used DS
166 optimization approach that has been used for various unconstrained problems. NMS uses an
167 iterative technique to generate a series of simplexes that converge to the best answer. When
168 solving an n-dimensional optimization issue, the NMS approach requires n+1 vertices to define
169 the beginning location of the simplex. To alter them simplex shape, you must do the following
170 operations in a single iteration: reflection, expansion, contraction, and reduction. This evolution
171 may continue in an unanticipated fashion, for example, with fewer iterations for a higher
172 number of choice variables, depending on the original simplex's starting position, shape, and
173 orientation [21].

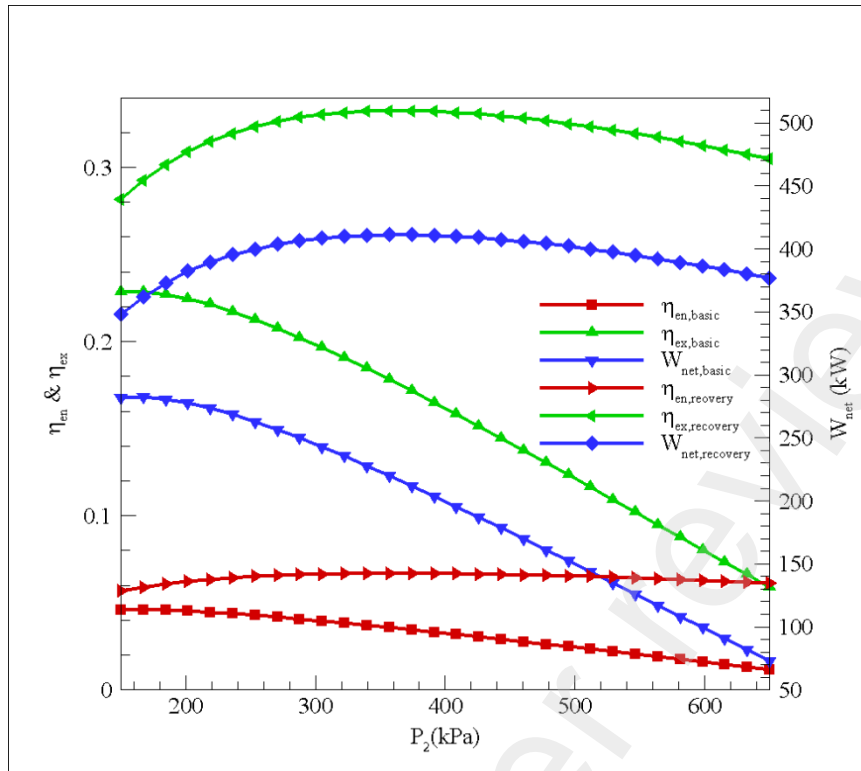
174 Table 2. Optimum parameters using different scenarios.

Parameters	Initial Mode	Optimal Mode using Genetic algorithm	Optimal mode using Nelder-Mead Simplex	Optimal Mode using Direct algorithm	Unit
Separator pressure	500	304.3	326.4	337.6	kPa
Carbon dioxide turbine inlet pressure	15000	13083	12067	12223	kPa

Steam Turbine exit pressure	20	37.36	22.01	30	kPa
Power production of steam turbine	150.1	194.2	218.1	200.6	kW
Power Production of carbon dioxide turbine	525.5	606.8	460.8	534.4	kW
Electric power consumption of pump 1	0.2436	0.2626	0.2762	0.2732	kW
Electric power consumption of pump 2	274.1	235.6	219	254.9	kW
Net power production	401.3	316	459.5	479.8	kW
Exergy efficiency	32.46	39.21	36.16	38.82	%

175 The total output of the output is 401.3 kW in BASIC mode, which after adding the recovery
176 cycle, this value reaches 316 kW in the optimized state with the genetic algorithm and 459.5
177 kW in the optimized form with the Nelder-Mead simplex method and 479.8 kW in the
178 optimized form with the Direct algorithm. Therefore, if the goal is to increase the net output
179 work, the working conditions obtained by the Direct algorithm have a better result.

180 According to Figure 4, the energy efficiency of the recovery power plant increases
181 monotonically as the separator pressure rises. In contrast, the trend for the energy efficiency of
182 the standalone geothermal power plant is downward because growing separator pressure raises
183 the geofluid-specific enthalpy of the production well. The effect of CO₂ condenser outlet
184 temperature on generated power, energy, and exergy efficiency is depicted in Figure 5. It shows
185 that a significant decrease in net power production is caused by raising the condenser outlet
186 temperature, yet none of these two efficiency losses is substantial. Given that the gas turbine
187 would provide less power, this is a logical outcome.

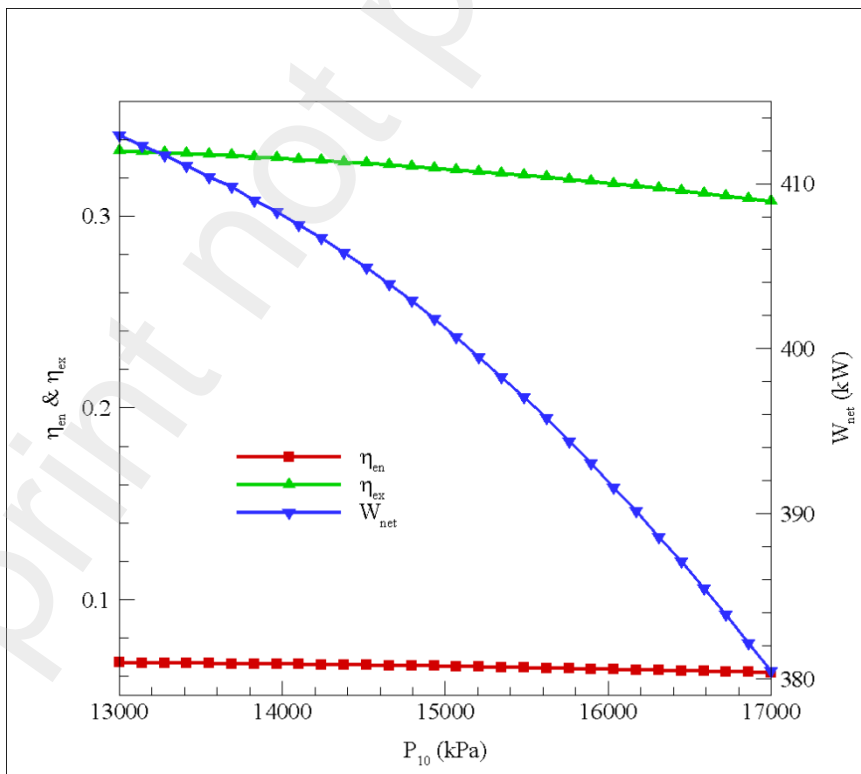


188

189 Figure 4. Energy and exergy efficiencies and net power output variation with separator

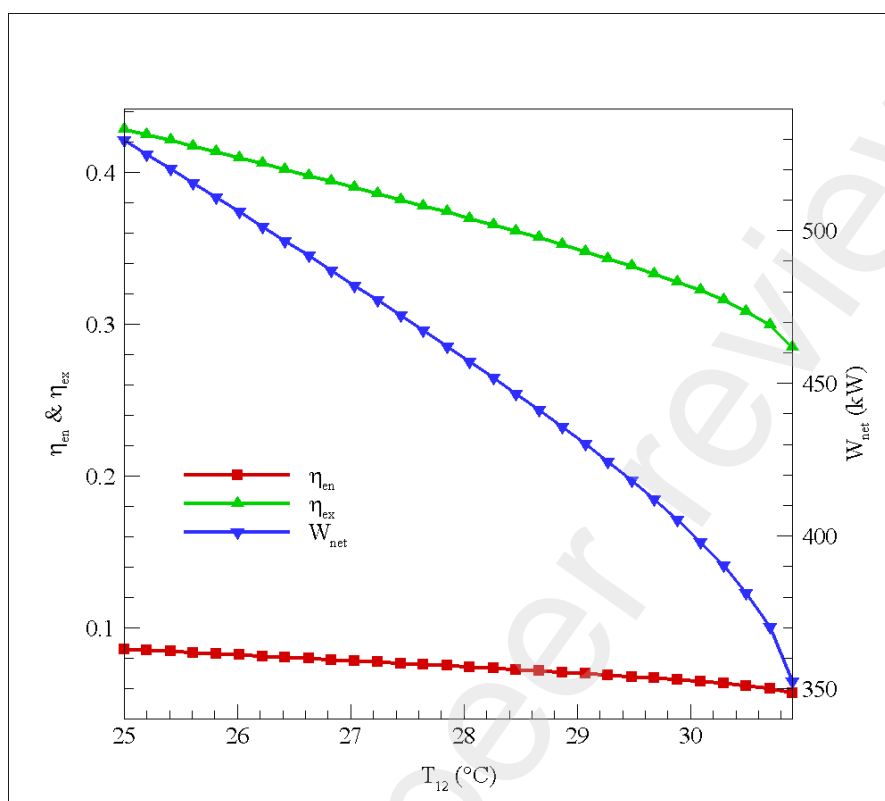
190

pressure for basic mode and recovery mode.



191

192 Figure 5. Energy and exergy efficiencies and net power output variation with CO₂ turbine
193 inlet pressure for recovery mode.



194
195 Figure 6. Energy and exergy efficiencies and net power output variation with CO₂ condenser
196 exit temperature for recovery mode.

197 Figure 6 depicts how a hybrid power plant's CO₂ turbine inlet pressure changes the net output
198 energy and accelerator efficiency. The findings indicate that the maximum values of the net
199 power output, exergy, and energy efficiencies occur at about 15 MPa. This can be explained
200 by the fact that raising the gas turbine's inlet pressure raises the inlet temperature of the gas
201 turbine, which increases the condenser's temperature (turbine outlet gas). As a result, the ideal
202 gas turbine inlet temperature is attained, enabling the hybrid power plant to run at its best
203 efficiency.

204

205 5. Conclusion

206 In this research, a combined power generation system (combined single-flash geothermal
207 system with trans-critical carbon dioxide cycle) in energy and exergy in both optimal and
208 primary states have been investigated and researched. Exergy efficiency in the initial state was
209 equal to 32.46%, and after the genetic Algorithm, this value increased to 39.21%. In the case
210 of the Nelder-Mead Simplex method, the exergy efficiency has increased from 32.46% to
211 36.16%. In the case of the Direct Algorithm, the exergy efficiency has increased from 32.46%
212 to 38.82%. The efficiency of using a genetic algorithm is more effective than other methods.

213 **References:**

- 214 [1] A.F. Zobaa, R.C. Bansal, Handbook of renewable energy technology, World
215 Scientific 2011.
- 216 [2] A. Kurchania, Biomass energy, Biomass Conversion, Springer 2012, pp. 91-122.
- 217 [3] N. Nordin, Limitations of Commercializing Fuel Cell Technologies, AIP Conference
218 Proceedings, American Institute of Physics, 2010, pp. 498-506.
- 219 [4] A.B. Karki, Biogas as renewable energy from organic waste, Biotechnology, 10 (2009) 1-
220 9.
- 221 [5] F. Liu, Y. Kang, Y. Hu, H. Chen, X. Wang, H. Pan, J. Xie, Comparative investigation on
222 the heat extraction performance of an enhanced geothermal system with N₂O, CO₂ and H₂O
223 as working fluids, Applied Thermal Engineering, 200 (2022) 117594.
- 224 [6] C. Sahana, S. De, S. Mondal, Integration of CO₂ power and refrigeration cycles with a
225 desalination unit to recover geothermal heat in an oilfield, Applied Thermal Engineering, 189
226 (2021) 116744.
- 227 [7] X. Wang, E.K. Levy, C. Pan, C.E. Romero, A. Banerjee, C. Rubio-Maya, L. Pan, Working
228 fluid selection for organic Rankine cycle power generation using hot produced supercritical
229 CO₂ from a geothermal reservoir, Applied Thermal Engineering, 149 (2019) 1287-1304.
- 230 [8] P.-X. Jiang, F.-Z. Zhang, R.-N. Xu, Thermodynamic analysis of a solar-enhanced
231 geothermal hybrid power plant using CO₂ as working fluid, Applied Thermal Engineering, 116
232 (2017) 463-472.
- 233 [9] T. Parikhani, M. Delpisheh, M.A. Haghghi, S.G. Holagh, H. Athari, Performance
234 enhancement and multi-objective optimization of a double-flash binary geothermal power
235 plant, Energy Nexus, 2 (2021) 100012.
- 236 [10] B. Melzi, N. Kefif, M.E.H. Assad, H. Delnava, A. Hamid, Modelling and Optimal Design
237 of Hybrid Power System Photovoltaic/Solid Oxide Fuel Cell for a Mediterranean City, Energy
238 Engineering, 118 (2021).
- 239 [11] T. Yazarlou, M.D. Saghafi, Investigation of Plans Shape and Glazing Percentage for the
240 Energy Efficiency of Residential Buildings, Energy Engineering, 118 (2021).
- 241 [12] N.A. Pambudi, S. Wibowo, Ranto, L.H. Saw, Experimental Investigation of Organic
242 Rankine Cycle (ORC) for Low Temperature Geothermal Fluid: Effect of Pump Rotation and
243 R-134 Working Fluid in Scroll-Expander, Energy Engineering, 118 (2021).
- 244 [13] P. Saengsikhiao, J. Taweekun, K. Maliwan, S. Sae-ung, T. Theppaya, Development of
245 Environmentally Friendly and Energy Efficient Refrigerants for Refrigeration Systems, Energy
246 Engineering, 118 (2021).

- 247 [14] J. Wang, J. Wang, Y. Dai, P. Zhao, Thermodynamic analysis and optimization of a flash-
248 binary geothermal power generation system, *Geothermics*, 55 (2015) 69-77.
- 249 [15] L. Chen, Y. Wang, M. Xie, K. Ye, S. Mohtaram, Energy and exergy analysis of two
250 modified adiabatic compressed air energy storage (A-CAES) system for cogeneration of power
251 and cooling on the base of volatile fluid, *Journal of Energy Storage*, 42 (2021) 103009.
- 252 [16] S. Mohtaram, Y. Sun, M. Omid, J. Lin, Energy-exergy efficiencies analyses of a waste-
253 to-power generation system combined with an ammonia-water dilution Rankine cycle, *Case
254 Studies in Thermal Engineering*, 25 (2021) 100909.
- 255 [17] A. Aali, N. Pourmahmoud, V. Zare, Exergoeconomic analysis and multi-objective
256 optimization of a novel combined flash-binary cycle for Sabalan geothermal power plant in
257 Iran, *Energy Conversion and Management*, 143 (2017) 377-390.
- 258 [18] M. El Haj Assad, Y. Aryanfar, A. Javaherian, A. Khosravi, K. Aghaei, S. Hosseinzadeh,
259 J. Pabon, S. Mahmoudi, Energy, exergy, economic and exergoenvironmental analyses of
260 transcritical CO₂ cycle powered by single flash geothermal power plant, *International Journal
261 of Low-Carbon Technologies*, 16 (2021) 1504-1518.
- 262 [19] H. Sun, Q. Dong, C. Zhang, J. Chen, An Energy Efficiency Improvement Method for
263 Manufacturing Process Based on ECRSR, *Energy Engineering*, 117 (2020).
- 264 [20] M.A. Ehyaei, A. Ahmadi, M.A. Rosen, A. Davarpanah, Thermodynamic Optimization of
265 a Geothermal Power Plant with a Genetic Algorithm in Two Stages, *Processes*, 8 (2020).
- 266 [21] P. Niegodajew, M. Marek, W. Elsner, Ł. Kowalczyk, Power Plant Optimisation—
267 Effective Use of the Nelder-Mead Approach, *Processes*, 8 (2020).

268